Research Article | Vol. 25, No. 9 | 1 May 2017 | OPTICS EXPRESS 10234
Optics EXPRESS

Synthesis, fabrication and characterization of a highly-dispersive mirrors for the 2 μm spectral range

TATIANA AMOTCHKINA,[1] MICHAEL TRUBETSKOV,[1] FLORIAN HABEL,[2] YURIJ. PERVAK,[3] JINWEI ZHANG,[1] KAFAI MAK,[1] OLEG PRONIN,[1] FERENC KRAUSZ,[1,2] AND VLADIMIR PERVAK[2]

[1]*Max-Planck-Institut für Quantenoptik, Hans-Kopfermann Str. 1, 85748 Garching, Germany*
[2]*Ludwig-Maximilians-Universität München, Am Coulombwall 1, 85748 Garching, Germany*
[3]*Taras Schevchenko Kiev National University, Volodymyrska str. 64, 01601, Kyiv, Ukraine*
[*]*Vladimir.Pervak@lmu.de*

Abstract: We report a challenging design, fabrication and post-production characterization problem of a dispersive mirror supporting the spectral range from 2000 nm to 2200 nm and providing a group delay dispersion of −1000 fs^2. The absolute reflectance in the working range is over 99.95%. The reported mirror is a critical element for Tm and Ho based lasers and paves the way for the development of ultrafast 2 μm lasers with sub-100 fs pulse duration.

OCIS codes: (310.4165) Multilayer design; (310.6845) Thin film devices and applications; (190.0190) Nonlinear optics; (320.0320) Ultrafast optics.

References and links

1. B. Stuart, *Infrared Spectroscopy: Fundamentals and Applications* (J. Wiley, 2004).
2. F. Stutzki, C. Gaida, M. Gebhardt, F. Jansen, C. Jauregui, J. Limpert, and A. Tünnermann, "Tm-based fiber-laser system with more than 200 MW peak power," Opt. Lett. **40**(1), 9–12 (2015).
3. I. T. Sorokina and E. Sorokin, "Femtosecond Cr2+ Based Lasers," IEEE J. Sel. Top. Quantum Electron. **21**(1), 273–291 (2015).
4. H. Pires, M. Baudisch, D. Sanchez, M. Hemmer, and J. Biegert, "Ultrashort pulse generation in the mid-IR," Prog. Quantum Electron. **43**, 1–30 (2015).
5. K. F. Mak, S. Groebmeyer, V. Pervak, F. Krausz, and O. Pronin, "Passively mode locked Ho:YAG oscillator at 2.1 μm," in *EUROPHOTON 2016* (2016), paper PO-3.30.
6. K. Yang, H. Bromberger, H. Ruf, H. Schäfer, J. Neuhaus, T. Dekorsy, C. V.-B. Grimm, M. Helm, K. Biermann, and H. Künzel, "Passively mode-locked Tm,Ho:YAG laser at 2 microm based on saturable absorption of intersubband transitions in quantum wells," Opt. Express **18**(7), 6537–6544 (2010).
7. E. Sorokin, I. T. Sorokina, M. S. Mirov, V. V. Fedorov, I. S. Moskalev, and S. B. Mirov, "Ultrabroad Continuous-Wave Tuning of Ceramic Cr:ZnSe and Cr:ZnS Lasers," in *Lasers, Sources and Related Photonic Devices* (OSA, 2010), paper AMC2.
8. V. O. Smolski, S. Vasilyev, P. G. Schunemann, S. B. Mirov, and K. L. Vodopyanov, "Cr:ZnS laser-pumped subharmonic GaAs optical parametric oscillator with the spectrum spanning 3.6-5.6 μm," Opt. Lett. **40**(12), 2906–2908 (2015).
9. D. Sanchez, M. Hemmer, M. Baudisch, S. L. Cousin, K. Zawilski, P. Schunemann, O. Chalus, C. Simon-Boisson, and J. Biegert, "7 μm, ultrafast, sub-millijoule-level mid-infrared optical parametric chirped pulse amplifier pumped at 2 μm," Optica **3**(2), 147 (2016).
10. Y. Chen, Y. Wang, L. Wang, M. Zhu, H. Qi, J. Shao, X. Huang, S. Yang, C. Li, K. Zhou, and Q. Zhu, "High dispersive mirrors for erbium-doped fiber chirped pulse amplification system," Opt. Express **24**(17), 19835–19840 (2016).
11. I. H. Malitson, "Interspecimen comparison of the refractive index of fused silica," J. Opt. Soc. Am. **55**(10), 1205–1208 (1965).
12. T. Amotchkina, H. Fattahi, Y. A. Pervak, M. Trubetskov, and V. Pervak, "Broadband beamsplitter for high intensity laser applications in the infra-red spectral range," Opt. Express **24**(15), 16752–16759 (2016).
13. A. V. Tikhonravov, M. K. Trubetskov, and G. W. DeBell, "Optical coating design approaches based on the needle optimization technique," Appl. Opt. **46**(5), 704–710 (2007).
14. A. V. Tikhonravov and M. K. Trubetskov, "OptiLayer software," http://www.optilayer.com.
15. V. Pervak, A. V. Tikhonravov, M. K. Trubetskov, S. Naumov, F. Krausz, and A. Apolonski, "1.5-octave chirped mirror for pulse compression down to sub-3 fs," Appl. Phys. B **87**(1), 5–12 (2007).

#287421 https://doi.org/10.1364/OE.25.010234
Journal © 2017 Received 23 Feb 2017; revised 7 Apr 2017; accepted 11 Apr 2017; published 25 Apr 2017

Optics EXPRESS

16. D. Ristau, H. Ehlers, T. Gross, and M. Lappschies, "Optical broadband monitoring of conventional and ion processes," Appl. Opt. **45**(7), 1495–1501 (2006).
17. F. Habel, M. Trubetskov, and V. Pervak, "Group delay dispersion measurements in the mid-infrared spectral range of 2-20 µm," Opt. Express **24**(15), 16705–16710 (2016).
18. H. A. Macleod, *Thin-Film Optical Filters*, 4th ed. (Taylor & Francis, 2010).
19. V. Pervak, "Recent development and new ideas in the field of dispersive multilayer optics," Appl. Opt. **50**(9), C55–C61 (2011).
20. V. Pervak, M. K. Trubetskov, and A. V. Tikhonravov, "Robust synthesis of dispersive mirrors," Opt. Express **19**(3), 2371–2380 (2011).
21. A. N. Tikhonov and V. I. Arsenin, *Solutions of Ill-Posed Problems* (Winston, 1977).
22. M. Trubetskov, T. Amotchkina, A. Tikhonravov, and V. Pervak, "Reverse engineering of multilayer coatings for ultrafast laser applications," Appl. Opt. **53**(4), A114–A120 (2014).
23. L. Gao, F. Lemarchand, and M. Lequime, "Exploitation of multiple incidences spectrometric measurements for thin film reverse engineering," Opt. Express **20**(14), 15734–15751 (2012).

1. Introduction

The mid-infrared fingerprint spectral region (2-20 µm) is important for numerous spectroscopy applications [1]. One promising scheme for generating coherent radiation in this region involves nonlinear conversion processes driven by emerging femtosecond fiber and solid-state lasers in 1.9-2.6 µm range [2,3]. Further development of these femtosecond driving lasers are therefore important for providing a more efficient mid-infrared source in a simpler manner [4].

One of the key elements of modern femtosecond lasers is dispersive mirror (DM). Although this technology is well established in the visible (~800 nm, Ti:Sa lasers) and near infrared range (~1030 nm, Yb:YAG lasers), its development at longer wavelengths beyond 1.9 µm is still at an early stage. As Thulium- and Holmium-based lasers operating at around 1.9-2.2 µm become more widespread [5,6], and the maturing of Cr:ZnS/ZnSe laser technology promises to extend laser output to 3.2 µm [3,7,8], there is an urgent need for DMs suitable for this spectral region. These mirrors will not only enable mode-locked femtosecond operation in next-generation Ho: YAG thin-disk oscillators, but also enable the extra-cavity compression of output from Ho-doped bulk amplifiers [9].

For dispersive mirrors to be useful, they need to satisfy three crucial criteria: high reflectance (>99.9%) and high negative group delay dispersion of −1000 fs^2. Production of such coatings for the 2 µm region is a challenge because coating layers for the infrared need to be thicker compared to those in the visible range, the absorption may affect mirror performance more strongly. Moreover, the material dispersion of the coatings' layers has to be known with high accuracy in this spectral range as well.

Recently, dispersive mirrors for a near infrared erbium-doped fiber chirped pulse amplification system have been developed (Ref [10]). The mirrors are designed and produced for the range from 1530 to 1575 nm with a GDD of −2000 fs^2. As GDD oscillations are unavoidable, a workaround was found: the mirrors were produced for two different reference wavelengths, which results in a slight offset of their spectra with respect to each other. Used together, the mirror pair provides a flat GDD.

In this paper, we concentrate on design, production and optical characterization of a dispersive mirror (DM) providing high reflectance and a group delay dispersion (GDD) of −1000 fs^2 in the range from 2000 nm to 2200 nm. Not only is this spectral range broader and deeper towards the infrared than [10], but more importantly, we achieved the required specification using only a single DM.

In Section 2 we demonstrate the feasibility of the complicated multilayer design in our production environment. In Section 3 we provide a comprehensive post-production characterization which helped us to correct the dispersion curve of the high refractive index material in the spectral range up to 2500 nm. This will allow a more accurate design for future DMs in this wavelength range. Our Conclusions are presented in Section 4.

Optics EXPRESS

2. Synthesis and fabrication

In our DM we used Ta_2O_5 and SiO_2 as the high and low index material respectively. We chose two types of substrates: B260 Glass (borosilicate glass) with a thickness of 1 mm and Suprasil (fused silica) with a thickness of 6.35 mm. *Nominal* dispersion curves of Ta_2O_5, B260 Glass and Suprasil refractive indices are described by the Cauchy formula:

$$n(\lambda) = A_0 + A_1\left(\frac{\lambda_0}{\lambda}\right)^2 + A_2\left(\frac{\lambda_0}{\lambda}\right)^4, \quad (1)$$

where A_0, A_1, A_2 are dimensionless parameters, $\lambda_0 = 1000$ nm, and λ is specified in nanometers. For Ta_2O_5 $A_0 = 2.065721$, $A_1 = 0.016830$, $A_2 = 0.001686$; for B260 Glass $A_0 = 1.51$, $A_1 = 5.254\cdot10^{-3}$, $A_2 = 6.328\cdot10^{-5}$; and for Suprasil $A_0 = 1.443268$, $A_1 = 0.00406$, $A_2 = 6.948\cdot10^{-6}$.

The dispersion behavior of SiO_2 is specified by the Sellmeier model [11] with coefficients determined in Ref [12]:

$$n^2 = 1 + \frac{B_1(\lambda/\lambda_0)^2}{(\lambda/\lambda_0)^2 - B_2} + \frac{B_3(\lambda/\lambda_0)^2}{(\lambda/\lambda_0)^2 - B_4} + \frac{B_5(\lambda/\lambda_0)^2}{(\lambda/\lambda_0)^2 - B_6}, \quad (2)$$

where $B_1,...,B_6$ are dimensionless parameters, $\lambda_0 = 1000$ nm, λ is specified in nanometers; $B_1 = 1.132952$, $B_2 = 0$, $B_3 = 0.020581$, $B_4 = 0.115406$, $B_5 = 3.448642$, $B_6 = 330.0719$.

The synthesis of DM was performed with the help of the needle optimization technique and gradual evolution algorithm incorporated into the OptiLayer software [13,14]. A merit function estimating the closeness of the designed spectral characteristics to the target specifications was defined as:

$$MF^2 = \sum_{i=1}^{801}\left(\frac{R_p(\mathbf{X},\lambda_i)}{\Delta_{1,j}}\right)^2 + \sum_{i=1}^{801}\left(\frac{GDD_p(\mathbf{X},\lambda_i)+1000}{\Delta_{2,j}}\right)^2, \quad (3)$$

where $\mathbf{X} = \{d_1,...,d_m\}$ is a vector of layer thicknesses, $\{\lambda_i\}$ are evenly distributed wavelength points in the spectral ranges from 2000 nm to 2200 nm; $\{\Delta_{1,j}\}$ and $\{\Delta_{2,j}\}$ are tolerances.

As a result, a 54-layer DM was synthesized. The total physical (geometrical) thickness of the coating is 15.9 mkm. Its thickness profile and theoretical GD/GDD are presented in Figs. 1(a) and 1(b), respectively.

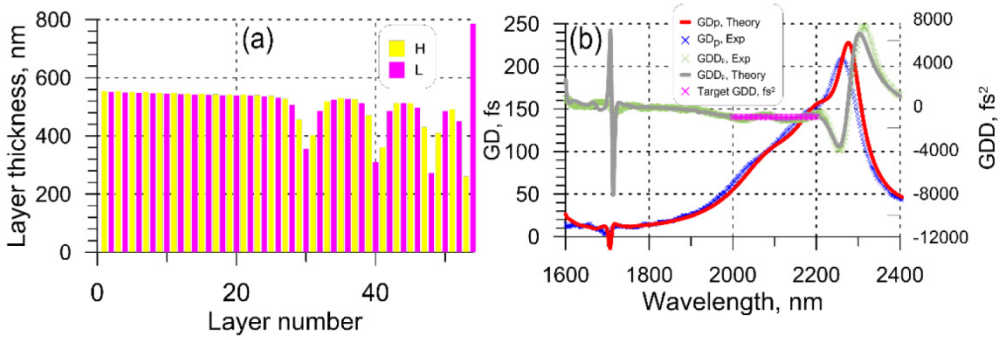

Fig. 1. (a) Thickness profile of the synthesized 54-layer DM, physical thicknesses are shown; (b) Comparison of theoretical and experimental GD/GDD related to DM-Suprasil sample.

Optics EXPRESS

The synthesized DM was fabricated using a Leybold Optics magnetron sputtering Helios plant, with the layer thicknesses controlled using well-calibrated time monitoring [15]. The plant is equipped with two proprietary dual-magnetrons and a plasma source for ion-assisted reactive middle frequency dual magnetron sputtering. The plant is also equipped with an optical broadband monitoring (BBM) system [16] which was used in a passive mode for data acquisition only. In the deposition run we used the Suprasil substrate for the DM fabrication and the cheaper B260 Glass substrate as a witness sample. As a result, two samples were obtained: DM coating on B260 Glass substrate (sample DM-B260) and DM coating on Suprasil substrate (DM-Suprasil). The transmittance scans (BBM data) after deposition of each layer except the last layer were recorded for the DM-B260 sample.

After the deposition, transmittance data of a DM-Suprasil sample was measured by a spectrophotometer (Perkin Elmer Lambda 950) in the range from 400 nm to 2500 nm. In order to reveal all the informative spectral features of the transmittance curves, the measurements were performed at 0.2 nm wavelength step and a spectral resolution of 0.5 nm (Fig. 2(a)). The measurement accuracy is better than 1%. The absolute reflectance in the range from 2030 nm to 2180 nm was measured by Layertec GmbH, Germany (Fig. 2(b)). It can be seen that the reflectance is above 99.9% across the spectral range, and is higher than 99.95% in the vicinity of the central wavelength (2050 nm). Indeed, reflectance values are only 0.04% lower than the theoretical curve, calculated without absorption in layer-established materials. The high measured reflectance is noteworthy given the significantly thicker dielectric layers in comparison to mirrors designed for 800 nm or 1030 nm. The GD and GDD measurements of the DM-Suprasil sample are shown in Fig. 1(b). They were extracted from data recorded by a mid-infrared white-light interferometer recently developed in-house [17]. The experimental data show that the produced DM satisfies the target specifications and can be used within a femtosecond laser oscillator.

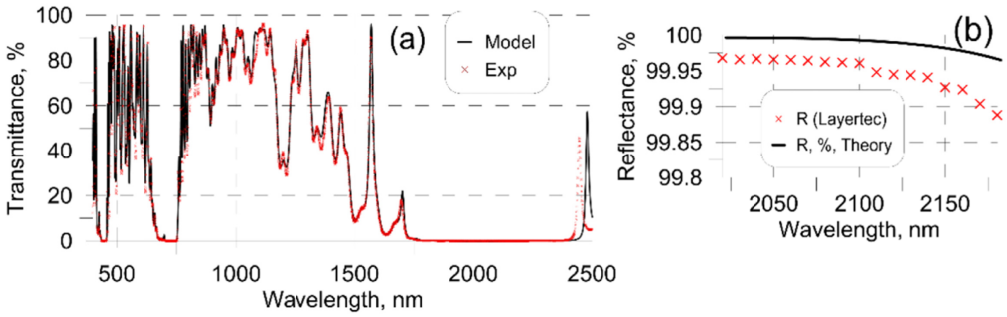

Fig. 2. (a) Comparison of the experimental and theoretical transmittance of the produced DM-Suprasil Sample; (b) Absolute reflectance of DM-Suprasil sample measured by Layertec and theoretical reflectance in the same spectral range.

3. Post-production characterization

In Fig. 2(a) one can observe that all spectral features of the theoretical spectral curve were reproduced by the experimental transmittance data. In addition, excellent correspondence between the measured and theoretical GD/GDD values (Fig. 1(b)) confirms the high accuracy of our deposition process. However, in the range between 1700 nm and 2500 nm, one can observe a small shift in the experimental transmittance with respect to the theoretical curve. The shift increases from 4 nm at 1700 nm (0.25%) to 12 nm at 2500 nm (0.5%). These deviations can be attributed to the inaccuracies in the refractive indices of the layer materials in the infrared spectral range. From thin film theory [18] it follows that the width of the high reflection zone is dependent on the ratio of high and low refractive indices. Since the width of the high reflection zone of the produced sample is narrower than the theoretical zone, one might assume that the nominal Ta_2O_5 index was overestimated. It means that careful

Optics EXPRESS

characterization of the produced samples should be performed in order to obtain a better estimate of the nominal Ta_2O_5 index.

As a first step of our characterization, we processed the BBM data (53 transmittance scans) in order to estimate the error in layer thicknesses. Keeping in mind that the expected errors are relatively small due to the high accuracy of time monitoring [19,20], we applied the algorithm assuming quasi-random errors in layer thicknesses [9,16]. The algorithm is based on the minimization of *in situ* Tikhonov's discrepancy function *TDF* with respect to the relative error δ_i, $i = 1,...,m-1$, m is the number of mirror layers:

$$TDF^2 = GDF^2 + \frac{\alpha}{m-1}\sum_{i=1}^{m-1}\delta_i^2, \quad GDF^2 = \frac{1}{(m-1)L}\sum_{i=1}^{m-1}\sum_{j=1}^{L}\left[T(\mathbf{X};\lambda_j) - \hat{T}^{(i)}(\lambda_j)\right]^2, \quad (4)$$

where $\mathbf{X} = \{d_1(1+\delta_1),...,d_i(1+\delta_i)\}$ is the vector of layer thicknesses of DM-B260 sample; $\{\lambda_j\}$ are evenly distributed wavelength points in the range from 400 nm to 950 nm; $L = 1239$. The last layer m is not included into this step, since the BBM device did not provide measurement data once the deposition is finished. The second term in Eq. (4) is responsible for the reliability of the solution by taking into account *a priori* information that expected random errors are-assumed to be quite low. This characterization approach is based on the Tikhonov's regularization theory of solving ill-posed problems [21]. In Eq. (4), α is a regularization parameter that provides a balance between data fitting and the stability of the characterization solution. In the present study, $\alpha = 1$. Initial *GDF* value was 6.83; in the course of optimization the value of 2.57 was achieved. Estimated errors δ_i do not exceed 2% that is agreed with expected accuracy of the time monitoring. Denote $\bar{d}_1 = d_1(1+\delta_1),...,\bar{d}_{m-1} = d_{m-1}(1+\delta_{m-1}),\bar{d}_m = d_m$ the thicknesses of the model coating obtained in this way.

In the second step of our characterization process, we searched for the actual layer thicknesses of the DM-Suprasil sample. As experimental data we considered *ex situ* transmittance measured in the visible spectral range from 400 nm to 860 nm. We introduced a discrepancy function *DF* in the standard way:

$$DF^2 = \frac{1}{L}\sum_{i=1}^{L}\left[T(\mathbf{X};\lambda_i) - \hat{T}(\lambda_i)\right]^2, \quad (5)$$

where $\mathbf{X} = \{\bar{d}_1 + \Delta,...,\bar{d}_{m-1} + \Delta, \bar{d}_m + \delta_m\}$ is the vector of layer thicknesses, Δ is a deviation between thicknesses of coating layers on B260 Glass and Suprasil substrates, δ_m is a random error in the last layer of the DM-Suprasil sample. We minimized the discrepancy function (Eq. (5)) with respect to two parameters, δ_m and Δ. The initial *DF* value was 16.4 and the *DF* value achieved in the course of the discrepancy function minimization was 5.72. The obtained Δ value of 0.1% is in a full agreement with the estimated thickness non-uniformity [22]. $\tilde{\mathbf{X}} = \{\bar{d}_1 + \Delta,...,\bar{d}_{m-1} + \Delta, \bar{d}_m + \delta_m\}$ denotes the vector of the determined layer thicknesses of the DM-Suprasil sample.

Comparing the transmittance of the design defined by the vector $\tilde{X}$ and the transmittance data measured from 860 nm to 2500 nm, we still observed a shift mentioned earlier. Therefore, as a third step of our characterization process the refractive index of Ta_2O_5 is corrected. We assumed that the refractive index of Ta_2O_5, $n_H(\lambda)$, in the broad range from 400 nm to 2500 nm can be described by the Cauchy formula, although this range is broader than the range from 400 nm to 1800 nm considered by the authors of Ref [23]. We optimized

Optics EXPRESS

the discrepancy function (Eq. (5)) in the wavelength range from 860 nm to 2500 nm with respect to three Cauchy parameters (see Eq. (1)), i.e., $\mathbf{X} = \{\tilde{d}_1, ..., \tilde{d}_m; A_0, A_1, A_2\}$. In order to obtain a refractive index of Ta_2O_5 in the whole spectral range from 400 nm to 2500 nm, we merged and subsequently smoothed the nominal index in the range from 400 nm to 860 nm and Ta_2O_5 refractive index in the range from 860 nm to 2500 nm estimated above. The corrected dispersion curve of Ta_2O_5 is shown in Fig. 3(a). The discrepancy function value (Eq. (5)) for the whole spectral range decreased from 8.61 to 4.74. It is seen from Fig. 3(a) that the wavelength dependence $n_H(\lambda)$ was almost unchanged in the visible spectral range in comparison with the nominal dispersion curve of Ta_2O_5.

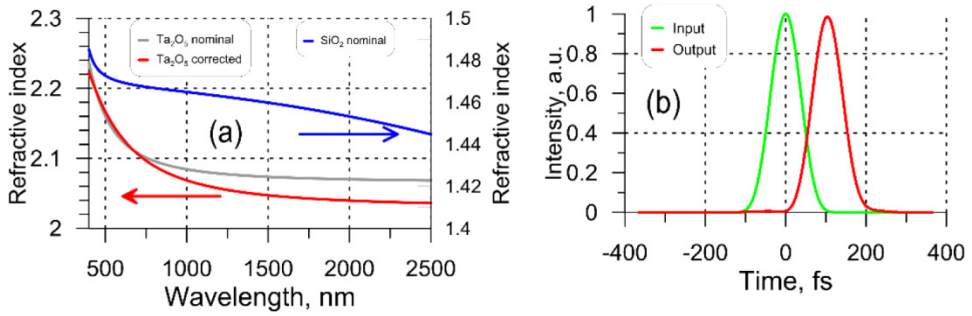

Fig. 3. (a) Comparison of the nominal and corrected refractive indices of Ta_2O_5; refractive index of SiO_2 is shown for information only; (b) Input (green) and output (red) pulse simulations. Output pulse is calculated after 10 reflections from the DM at AOI = 5°with subtracted GDD target.

As the last step of our characterization process we validated the results with the help of GD/GDD measurements. Instead of experimental and model transmittance, we substituted GD/GDD measurement and theoretical data into Eq. (5) and calculated the initial values of the discrepancy function DF in the spectral range from 1600 nm to 2400 nm with $L = 540$. The achieved value of the discrepancy function can be calculated with GD/GDD experimental and model data substituted into Eq. (5). In the case of GD, initial DF was equal to 687.3 and achieved value was 411.3. In the case of GDD, initial DF was equal to 115110.0 and achieved value was 97447. The decreases of DF values after replacement of the theoretical design by the model, indicate the reliability of the obtained results.

In Fig. 3(b) the simulated envelopes of the input Fourier-limited pulse and the pulse reflected from the DM with subtracted GDD are presented. The input pulse has pulse duration of 87 fs and a super-Gaussian spectrum with bandwidth of 15 THz. One can observe that the shape of the reflected pulse is close to the Fourier-limit. The duration of reflected pulse remains unchanged even after 10 bounces of reflection.

4. Conclusions

A broadband highly dispersive mirror for Thulium and Holmium lasers has been successfully synthesized and characterized. The absolute reflectance reaches up to 99.95%, which allows their applications inside laser oscillators that are sensitive to mirror losses. Excellent spectral performance as well as proven group delay dispersion enable its application in extra-cavity temporal pulse-compression and intracavity dispersion compensation in next generation 2 µm thin-disk oscillators.

Funding

This work was supported by the DFG Cluster of Excellence, "Munich Centre for Advanced Photonics," (www.munich-photonics.de). T. Amotchkina has received funding from the

Optics EXPRESS

European Union's Horizon 2020 research and innovation programme under the Marie Skłodowska-Curie agreement No 657596.